Electromagnetic Formulations for HTS Coated Conductors and HTS Tape Topologies Using the Finite Element Method

Diogo José Gameiro Carvalho

diogojgameiro@gmail.com
Instituto Superior Técnico, Lisboa

***Abstract*—FEM simulation of HTS-CC and HTS tape topologies is of great interest in several applications, from power systems, to health, and to physics and engineering research. Different electromagnetic formulations have been used and implemented in FEM to simulate HTS-CC and HTS tape topologies, which are typically demanding in computational resources, specifically regarding computation time. Recently, mixed formulations using a combination of different formulations have been proposed, showing to be considerably faster than conventional formulations. Different formulations present distinct behaviors and characteristics, depending on the simulation conditions, as well as the geometry and HTS model used. This thesis presents a review of the electromagnetic formulations proposed in the literature for FEM simulation of HTS-CC and HTS tape topologies, focusing on their implementation. Moreover, implementation aspects, which are lacking in the literature, are also proposed, specifically for the $T-A$ and $T-\phi$ formulations. Additionally, FEM simulations are developed for relevant HTS-CC and HTS tape topologies, considering the formulation implementations studied. The simulation results are analyzed, alongside the consequent conclusions regarding advantages and disadvantages, as well as strengths and limitations, for each formulation, considering each geometry and simulation conditions. The $T-A$ formulation has shown to be the most interesting to be used in FEM simulations of HTS tape topologies, being considerably more computationally resource efficient than other conventional formulations. Accordingly, FEM simulations are developed for two HTS tape topologies, the HTS TSTC and CORC cables, using the $T-A$ formulation, whose results are also discussed.**

***Index Terms*—High-Temperature Superconductors (HTS), HTS Coated Conductors (HTS-CC), HTS Tape Topologies, Electromagnetic Formulations, Finite Element Method (FEM)**

I. Introduction

High-Temperature Superconducting Coated Conductors (HTS-CC) and High-Temperature Superconductor (HTS) tape topologies are of great interest in practical applications [1]–[3], from power systems, e.g. Superconducting Magnetic Energy Storage (SMES) systems, motors and generators, transformers, and fault current limiters, to health, e.g. high-resolution Magnetic Resonance Imaging (MRI) and Nuclear Magnetic Resonance (NMR) systems, to physics and engineering research, e.g. high-energy particle accelerators and nuclear fusion reactors (as the tokamak).

A. HTS Coated Conductors

HTS materials, as YBCO and BSCCO, were first synthesized in the bulk form. However, ever since the discovery of HTS, several techniques were developed for HTS wires and tapes manufacture. HTS wires and tapes, as well as their respective fabrication processes, can be divided in two categories (generations): First Generation (1G) HTS multi-filament composite, which are currently in the stage of medium-term commercialization; and Second Generation (2G) HTS-CC composite, which are currently in the early commercialization stage.

1G HTS tapes and wires using the PIT technique with BSCCO have been manufactured with lengths of about two kilometers. However, given their limited mechanical properties, as well as their critical current density depreciation under high magnetic fields, alternative manufacturing techniques have been under intense research.

2G HTS tapes correspond to a stack of layers of different materials, each one having a specific function. A commercial ReBCO 2G HTS-CC manufactured by Super Power Inc. and its layer constitution is schematically represented in Figure 1 [4].

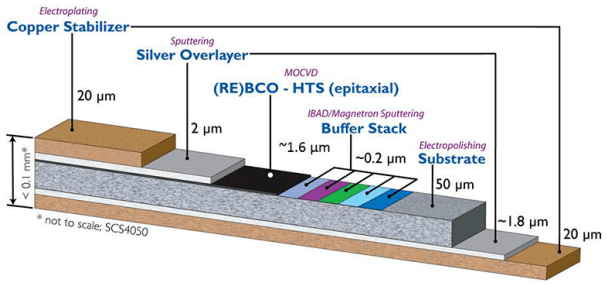

Figure 1: Super Power Inc. ReBCO 2G HTS SCS4050 layer constitution representation [4]

In general, high-current HTS cables are required for the referred practical applications. Current capacities of HTS tapes can be increased with the association of multiple parallel connected conductors. However, if connected in a simple topology, e.g. a tape stack, magnetic flux coupling (self-field effects) between conductors may lead to current unbalances, given the discrepancy between the values of the critical current I_c through different conductors. In order to address this issue, HTS cables are typically manufactured in a transposed design, which means that along a cable, each tape will eventually occupy all the positions previously occupied by all the other. Different HTS-CC cabling (topologies) have been proposed

and developed, such as Roebel Assembled Coated Conductor (RACC), Coated Conductor Rutherford Cable (CCRC), TSTC, CORC, as well as variations of these.

B. HTS-CC and HTS Tape Topologies Simulation

HTS materials are costly and the fabrication processes used to manufacture HTS-CC are typically very demanding. Consequently, HTS-CC and HTS tape topologies are expensive, which, in turn, compromises the development of research prototypes of systems including HTS-CC, given the typical limited funding available.

One way of overcoming this issue is to develop and study such prototypes in a simulation environment, i.e. through the simulation of the HTS tape topologies of interest using computer-based numerical methods. However, HTS-CC systems of interest are typically complex in geometry and their simulation models are usually described by a highly non-linear behavior, which complicate the analysis and weigh on the computational methods.

The most widely-used method to simulate electromagnetic problems corresponds to the Finite Element Method (FEM), which has shown to be very robust and versatile to deal with complex geometries and material models represented by non-linear characteristics, as it is the case of typically used models for HTS materials.

Accordingly, different ways of expressing the fundamental Maxwell's electromagnetism equations, i.e. electromagnetic formulations, can be used in FEM to simulate such HTS tape topologies.

Traditionally, the magnetic field H and the magnetic vector potential A formulations are the ones used to solve general electromagnetic problems in FEM. Recently, with the objective of reducing the computational requirements to solve problems containing HTS materials (mainly computation time and memory), combinations of formulations have been proposed and implemented, using mixed formulations between the H [5], [6], A [7], [8], as well as the magnetic scalar potential ϕ and the current vector potential T formulations, namely the $H-A$ [9], [10], $H-\phi$ [11], [12], $T-A$ [13], [14], and $T-\phi$ mixed formulations.

These formulations have different characteristics and distinct behaviors while solving electromagnetic problems containing HTS-CC in FEM, being suited for different types of geometries and simulation conditions. A more precise and detailed study on these formulations is needed, particularly in the scope of specific HTS tape topologies used in practical applications, such as the TSTC and CORC cables.

II. Electromagnetic Formulations

The starting point of any electromagnetic field problem are the well-known Maxwell's equations, constituting the foundation of any electromagnetic formulation, which corresponds to a specific way to write said equations with the objective of finding a solution to the field quantities, generally $\mathbf{B}$ and $\mathbf{H}$, as well as $\mathbf{E}$ and $\mathbf{J}$.

Although it is possible to obtain analytical solutions for some of these problems, for others, more complex, e.g. modelled by non-linear relations and/or with complicated geometries, analytical solutions may not usually be obtainable. Therefore, numerical methods arise as robust and useful alternatives to solve such problems, with the Finite Element Method (FEM) being one of the most versatile and studied.

Different formulations, using different state variables have been proposed and used to solve electromagnetic problems using FEM. The formulations' state variables may be the direct field quantities or their potentials, scalar or vector, as it is described below.

Several mixed formulations have been proposed, specifically to model electromagnetic problems containing HTS materials, where the choice of a formulation is a key factor. In a mixed formulation, two or more formulations are used to model different materials, i.e. domains Ω.

Typically, the H and T formulations are used to model the HTS domains Ω_{HTS}, since they can better handle the non-linear HTS model. The A formulation is generally used to model the non-HTS domains, such as dielectric (e.g. air) and ferromagnetic (e.g. iron) materials. The ϕ formulation is used to model non-conducting domains, since the major assumption of this formulation is the non-existence of currents.

In this Section, the HTS electromagnetic model used and the formulations studied, namely the H, A, $H-A$, $H-\phi$, $T-A$, and $T-\phi$, as well as some relevant aspects of the respective FEM implementations (in a commercially available FEM software) are described.

A. HTS Electromagnetic Model

HTS are used in real applications in the mixed state. As such, the mixed state of HTS will be the subject of analysis, regarding their electromagnetic modelling.

The most widely used model to describe the mixed state of macroscopic samples of HTS materials, including HTS commercial tapes, corresponds to the $E-J$ power law, alongside Bean's critical state model with Kim's empirical proposal for the J_c dependence with the magnetic flux density norm B, i.e.

$$\mathbf{E}(\mathbf{J}) = E_0 \left(\frac{J}{J_c(B)} \right)^n \frac{\mathbf{J}}{J}, \tag{1}$$

where

$$J_c(B) = J_{c0} \frac{B_0}{B_0 + B}. \tag{2}$$

Taking into consideration this HTS model, a HTS resistivity ρ_{HTS}, as a function of B and J, can be derived making a parallelism with Ohm's law,

$$\rho_{HTS}(B, J) = \frac{E_0}{J_{c0}} \left(\frac{B_0 + B}{B_0} \right)^n \left(\frac{J}{J_{c0}} \right)^{n-1}. \tag{3}$$

This model is the one used to simulate HTS-CC in this work, with the model parameters being typical ones for 2G HTS tapes, presented in Table I.

Regarding the geometry of the HTS-CC to be used, a common approximation is done from typical HTS-CC, as the one presented in Figure 1, where the HTS layer is considered to fill the whole tape thickness, i.e. $h_{HTS} = h_{tape} = 95.6\,\mu\text{m}$.

Table I: Electromagnetic model parameters for a representative 2G HTS tape

n	21
E_0	$100\,\mu\mathrm{V\,m^{-1}}$
J_{c0}	$\frac{1.6}{95.6} \times 2 \times 10^{10}\,\mathrm{A\,m^{-2}}$
B_0	$100\,\mathrm{mT}$

Naturally, the J_{c0} parameter from the HTS model is corrected to ensure the typical critical current of such tape, i.e. $I_c = 120\,\mathrm{A}$. Moreover, the width of the HTS tape considered in this work corresponds to $w_{tape} = 4\,\mathrm{mm}$. A schematic representation of the full and simplified models layers is presented in Figure 2.

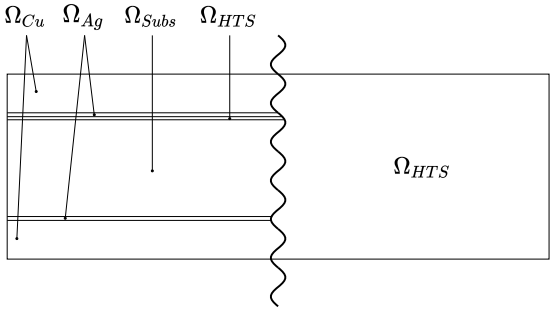

Figure 2: Schematic representation of the full (left) and simplified (right) models layers

B. H Formulation

The Magnetic Field formulation, usually called H formulation, corresponds to the formulation using the magnetic field $\mathbf{H}$ as state variable.

The vector field equation to be solved corresponds to the Faraday's law,

$$\nabla \times (\rho \nabla \times \mathbf{H}) = -\mu \frac{\partial \mathbf{H}}{\partial t}, \tag{4}$$

considering, using the Ampère's and Ohm's laws,

$$\mathbf{E} = \rho \nabla \times \mathbf{H}, \tag{5}$$

which can be written with respect to the magnetic field $\mathbf{H}$, specifically ρ.

The FEM software implementation of the H formulation is done straightforwardly using the *General Form PDE* module.

Additionally, an applied magnetic field and an applied transport current constraints can be respectively implemented using a *Dirichlet* boundary condition and a *Pointwise* constraint, by defining the integral of the current density, as

$$\int_S \mathbf{J} \cdot \mathbf{n}\ dS - I_{ap} = 0. \tag{6}$$

The shape function type used for the state variable $\mathbf{H}$ corresponds to a *Curl* element, also called edge element.

C. A Formulation

The Magnetic Vector Potential formulation, usually called A formulation (also refereed to as $A-\phi$ or $A-V$ formulation), corresponds to the formulation traditionally used in magnetic fields problems.

The foundation of the A formulation is the Gauss' law for magnetism, stating the divergence-free property of the magnetic flux density $\mathbf{B}$. The state variable $\mathbf{A}$ is defined as

$$\mathbf{B} = \nabla \times \mathbf{A}. \tag{7}$$

The vector field equation solved by this formulation is derived from the Maxwell's equations and from the previous definition for $\mathbf{A}$, alongside some considerations regarding gauge fixing, corresponding to

$$\nabla^2 \mathbf{A} = \mu\sigma \frac{\partial \mathbf{A}}{\partial t}. \tag{8}$$

It is important to notice that, in some problems, the right-hand side of (8) can be substituted by a current density source.

The FEM software implementation of the A formulation is done using the *Magnetic Fields* module, which is built specifically to solve the A formulation. Additionally, an applied magnetic field constraint can be implemented recurring to a *Magnetic Field* boundary constraint.

The shape function type used for the state variable $\mathbf{A}$ corresponds to a *Lagrange* element, being the most standard widely used shape function type.

D. $H - A$ Formulation

The mixed Magnetic Field - Magnetic Vector Potential formulation, usually called $H-A$ formulation, corresponds to the formulation where the H formulation is solved in Ω_{HTS} and the A formulation is solved in the remaining domains. Each formulation is solved and implemented in FEM software as described in Sections II-B and II-C, respectively.

In the $H-A$ formulation, boundary constraints have to be considered and implemented in FEM software to couple both formulations across the respective boundaries, thus solving the whole problem. Therefore, in the shared boundaries, the continuity of the tangential components of $\mathbf{E}$ and $\mathbf{H}$ are respectively constraint by means of a *Flux/Source* boundary constraint in the H formulation side and a *Magnetic Field* boundary constraint in the A formulation side.

In addition, an applied magnetic field constraint in the A formulation and an applied transport current constraint in the H formulation can be implemented as described in Sections II-B and II-C, respectively.

The shape function used for both state variables $\mathbf{H}$ and $\mathbf{A}$ corresponds to a *Lagrange* element.

E. $H - \phi$ Formulation

The mixed Magnetic Field - Magnetic Scalar Potential formulation, usually called $H-\phi$ formulation, allows for a reduction in complexity of electromagnetic problems where HTS materials are surrounded by non-conducting domains.

The H formulation is solved in Ω_{HTS} as described in Section II-B, alongside its FEM software implementation. The

ϕ formulation is solved in non-conducting domains, since its fundamental aspect is the non-existence of current, which allow to solve $\mathbf{H}$ by means of the magnetic scalar potential ϕ, being defined as

$$\mathbf{H} = -\nabla\phi. \tag{9}$$

The equation solved in the ϕ formulation, being implemented in FEM software using the *Magnetic Fields Without Currents*, corresponds to the Gauss' law for magnetism, alongside the considerations of a linear and isotropic medium, i.e.

$$\mu\nabla^2\phi = 0. \tag{10}$$

The boundary constraints to be implemented in FEM software to couple the H and ϕ formulations correspond to the continuity of the magnetic field $\mathbf{H}$ across the shared boundaries, specifically the continuity of the tangential components in the H formulation side, and the continuity of the normal components in the ϕ formulation side. This is done using a boundary *Constraint* in the H formulation and a *Magnetic Flux Density* boundary constraint in the ϕ formulation.

In addition, an applied magnetic field constraint in the ϕ formulation can be implemented using a *Magnetic Flux Density* boundary constraint and an applied transport current constraint can be implemented in the H formulation as described in Section II-B, alongside the consideration of the thin cut in the ϕ formulation domain Ω_ϕ, allowing for a discontinuity ϕ_d in the scalar field ϕ in accordance with such current constraint, defined as

$$I = \phi_d = \phi_d^+ - \phi_d^-, \tag{11}$$

as schematically represented in Figure 3, where l_1 and l_2 correspond to two possible closed paths in Ω_ϕ where the Ampère's law (alongside Stokes' theorem) can be used to compute the current in Ω_H.

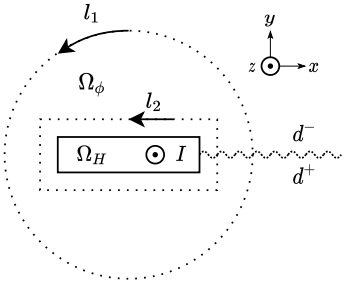

Figure 3: Schematic representation of an HTS tape cross section with transport current and the magnetic scalar potential discontinuity

The shape function type used for the state variables $\mathbf{H}$ and ϕ correspond to *Curl* and *Lagrange* elements, respectively.

F. $T - A$ Formulation

In the mixed Current Vector Potential - Magnetic Vector Potential formulation, usually called $T-A$ formulation, the $\mathbf{T}$ field is solved as the state variable in Ω_{HTS}, which correspond to surfaces, and the $\mathbf{A}$ field is solved as the state variable in all remaining domains. In this formulation, the HTS tape thickness is neglected, and, as a consequence, currents are constraint to exist only in a surface representing the HTS tape.

The A formulation is solved and implemented as described in Section II-C. In Ω_{HTS}, the $\mathbf{T}$ state variable, defined as

$$\mathbf{J} = \nabla \times \mathbf{T}, \tag{12}$$

is solved, being a vector field normal to the HTS surface, described by

$$\mathbf{T} = T\mathbf{n}_s, \tag{13}$$

which, in fact, corresponds to solve a scalar field T in Ω_{HTS}, by using the surface's unit normal vector $\mathbf{n}_s$.

The T formulation is implemented in FEM software in the *General Form Boundary PDE* module, in which an equivalent equation system to the H formulation is implemented, with the difference being the definition of the current density $\mathbf{J}$ (12).

In what regards the formulations coupling, in the T formulation, the magnetic flux density field $\mathbf{B}$ solved by the A formulation is considered as a source to the equation system (right-hand side of (4)), while in the A formulation, a *Surface Current Density* constraint is considered to ensure a corresponding discontinuity of $\mathbf{H}$ (specifically in its tangential components) across the HTS surface, in accordance with $\mathbf{J}$ solved in the T formulation.

Additionally, an applied magnetic field constraint can be implemented in the A formulation as described in II-C. An applied transport current constraint can be implemented in the T formulation by specifying *Dirichlet* boundary conditions in appropriate HTS domains boundaries Γ_{HTS}, following the application of Stokes' theorem to the computation of the current in a cross section of the HTS tape, i.e.

$$I = \delta\left(T_1 - T_2\right), \tag{14}$$

with T_1 and T_2 being the values specified by the *Dirichlet* boundary conditions and δ representing the real thickness of the tape.

A schematic representation of the thin sheet approximation, as well as the boundaries Γ_{HTS} where the *Dirichlet* boundary conditions stated in (14) are considered, is presented in Figure 4.

The shape function type used for the state variables $\mathbf{T}$ and $\mathbf{A}$ correspond to *Lagrange* elements.

G. $T - \phi$ Formulation

In the mixed Current Vector Potential - Magnetic Scalar Potential formulation, usually called $T-\phi$, the T formulation is solved in the Ω_{HTS} (modeled as thin sheets) and the ϕ formulation is solved in the remaining, non-conducting, domains. Each formulation is solved and implemented in FEM software as described in Sections II-F and II-E, respectively.

The boundary constraints to be implemented in FEM software to couple the T and ϕ formulations correspond, in the ϕ formulation to the discontinuity of the tangential components magnetic field $\mathbf{H}$ across the HTS surface, considering the surface current density in Ω_{HTS}. Moreover, a ϕ discontinuity is defined in Ω_{HTS} to allow for the existence of current in said surface. In the T formulation, similarly to what is described

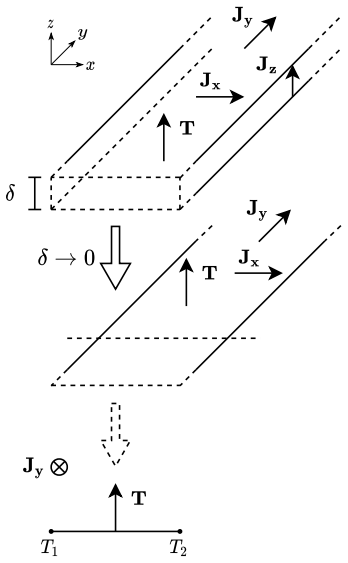

Figure 4: Schematic representation of the thin sheet approximation of a tape, alongside $\mathbf{J}$ and $\mathbf{T}$

in Section II-F, a magnetic field source corresponding to the magnetic field solved by the ϕ formulation is considered within the solved equation system for T.

In addition, an applied magnetic field constraint in the ϕ formulation and an applied transport current constraint in the T formulation can be implemented as described in Sections II-E and II-F, respectively.

The shape function type used for the state variables $\mathbf{T}$ and ϕ correspond to *Lagrange* elements.

H. Periodic Boundary Conditions

In addition to what is discussed before regarding each formulation implementation, and only in 3D geometries, *Periodic Condition* constraints may be added, for example to model a small portion of an infinitely-repeating geometry, as it is the case of the cable geometries considered in this work.

In the case of boundaries corresponding to the H formulation, *Elemental Periodic Condition* constraints are considered in the *General Form PDE* module.

In other formulations, as it is the case of the A and ϕ formulations, the natural boundary conditions applied by default, alongside all other added constraints, are enough to completely define the problem and allow the determination of the intended unique solution in geometries with specific symmetries, for example in the case of TSTC cable.

In other, more complex, geometries, the natural boundary conditions and other added constraints are not enough to ensure the determination of the intended solution. However, for the HTS tape topologies considered in the work developed, the *Periodic Condition* constraints available have shown to be ineffective, and no methods to overcome this issue were found in the literature. Nevertheless, a solution truncation method is used to simulate such topologies, specifically a CORC cable.

In addition, in what respects the T formulation, solved by the *General Form Boundary PDE* module, *Periodic Condition* constraints are disregarded, not only because the module has no such type of constraint available, but also because its implementation using alternative methods was neither proposed in the literature nor developed in the course of this work.

III. Finite Element Simulations

In this thesis, the different electromagnetic formulations and respective FEM software implementations were evaluated for a single HTS tape and an HTS tape stack. For both topologies, 2D and 3D geometries were studied and two simulations were conducted, namely applied magnetic field and applied transport current.

Afterwards, applied transport current simulations were developed in 3D geometries for two HTS tape cable topologies, TSTC and CORC cables. These simulations are the ones presented in this Section, as they are the most typically interesting for practical applications.

Temperature and Material Properties: In all simulations, the temperature is considered to be kept constant at $T = 77\,\mathrm{K}$, i.e. isothermal conditions are assumed. Moreover, in all material domains, including the HTS domains, the magnetic permeability is considered to be $\mu = \mu_0 = 4\pi \times 10^{-7}\,\mathrm{H\,m^{-1}}$.

In all geometries simulated, the only materials considered correspond to air and HTS materials, i.e. HTS tapes involved in air. The electric resistivity of the air domains Ω_{air} is set at $\rho_{air} = 1\,\Omega\,\mathrm{m}$, as it is considered to be sufficiently low to guarantee the convergence of the numerical method, but high enough to obtain accurate results of all the field quantities in Ω_{air}, while the resistivity of the HTS domains Ω_{HTS} is set as ρ_{HTS} as specified in (3).

Finite Element Discretization: The shape functions types used in all proposed formulations are the ones stated in Section II. Moreover, in all FEM simulations developed, the order of the elements corresponds to quadratic for the H, A, and ϕ state variables, and linear for the T state variable. The only exception corresponds to the order of the H domain $Lagrange$ elements used in the mixed $H - A$ formulation, which are set as linear elements.

These choices regarding the shape functions type and order, more than the common choices taken in the formulation implementations proposed in the literature, are the ones that deliver a adequate balance between solution accuracy and speed.

Moreover, the mesh is developed in the FEM software to, while ensuring convergence, balance the method accuracy with computational and convergence speed. Additionally, triangular and tetrahedral mesh elements are used respectively in 2D (Ω_{HTS}) and 3D (Ω_{air}) domains, with the exception of the $T-\phi$ formulation Ω_{HTS}, where quadrangular mesh elements are used.

A. Implemented Simulations

For the proposed HTS tape topologies, two simulations are conducted, namely applied magnetic field H_{ap} (or magnetic flux density B_{ap}, depending on the formulation used) and applied transport current I_{ap} (with no applied magnetic field).

In the implemented applied transport current I_{ap} simulation, a sinusoidal current with a frequency of $f = 50\,\mathrm{Hz}$ and

amplitude I_{ap}^{max} is constraint in the HTS tapes' domains. The simulation time is chosen to be two periods of the applied transport current, i.e. $t_{sim} = 40\,\mathrm{ms}$, since a steady state regime is verified after one period.

In the applied magnetic field simulation, a magnetization pulse perpendicular to the tape is constraint in the air outer boundary as a pulse with a duration of $t_{sim} = 20\,\mathrm{ms}$ and an amplitude of B_{ap}^{max}.

In the simulations conducted, the initial conditions correspond to the zero solution. Consequently, all field quantities, as well as the externally applied transport current signal start in zero.

The relative tolerance is set at $\epsilon = 1 \times 10^{-4}$ and the maximum time step constraint is defined at $\Delta t_{max} = 0.2\,\mathrm{ms}$. Moreover, in all simulations conducted, the FDM and the direct linear equation system solver used correspond to the BDF and to the MUMPS, respectively.

The simulations proposed were implemented in the FEM software on an Asus® laptop with an Intel® Core™ i9-11900H processor and 32 GB of random access memory, running version 21H2 of Windows 11® Home operating system.

All FEM software model files for all topologies and simulations developed are publicly available online in a Google Drive folder[1].

Simulation Results: In what respects the simulation results, in addition to the field distributions, specifically of the magnetic flux density $\mathbf{B}$ and critical current density $\mathbf{J}$, results regarding the formulations metrics, such as number of mesh elements and DOFs, RAM memory usage, and simulation computation time are matter for analysis.

Given the limited space available, the mentioned field distributions for all simulations are publicly available online in a Google Drive folder, only for three different simulation time instants, considered to be the most relevant for analysis.

Finally, the mean value of the instantaneous Joule losses per cable unit length P, defined in 3D geometries as

$$P = \frac{1}{l_{tape}} \int_{\Omega_{HTS}} \mathbf{E} \cdot \mathbf{J} \; d\Omega_{HTS}, \tag{15}$$

is also analyzed for each topology, simulation, and formulation. To be noted that in the T-based formulations the P value computed as described in (15) must be multiplied by the tape thickness h_{tape}.

B. HTS Tape Stack

The HTS tape stack topology corresponds to a six HTS tape stack immersed in air. Both 2D and 3D geometries are studied. The implementation under FEM software of the six formulations is described in Section II.

The HTS tape stack geometry implemented in FEM software corresponds to a portion of an infinitely-long tape stack with width and thickness as previously stated and with a length of $l_{tape} = 2\,\mathrm{cm}$. Moreover, each HTS tape is separated by air from the corresponding neighbors by a distance of $d_{tapes} = 2h_{tape} = 191.2\,\mu\mathrm{m}$. A cylinder (or a circle in the 2D geometry) with a radius of $r_{air} = 1\,\mathrm{cm}$ and centered in the geometric center of the stack is used to involve the stack in air.

Two different simulations are implemented, namely applied magnetic field B_{ap} (with no applied transport current), with $B_{ap}^{max} = 0.5\,\mathrm{T}$, and applied transport current I_{ap} (with no applied magnetic field), with $I_{ap}^{max} = 0.8 \times 6 \cdot I_c = 614.4\,\mathrm{A}$.

The behavior of both magnetic flux density distribution in Ω_{air} and current density distribution in Ω_{HTS} results are similar to the ones expectedly verified in HTS bulks, i.e. a behavior as in the single HTS tape simulation, but where each tape now suffers the effect of all other. Additionally, these results regarding field distributions show a good agreement between formulations.

However, results regarding the current density distributions in the applied transport current simulation show some deviations between formulations, specifically between the H-based and T-based formulations. In fact, a simplified HTS tape model is used in the H-based formulations geometries, which impacts the accuracy of the current density distribution results. It must be noted that the results that are considered to be more accurate, given the thin sheet approximation, correspond to the ones from the T-based formulations.

In addition, the instantaneous Joule losses P results, also show similar solutions across formulations, for both applied magnetic field and applied transport current simulations.

The applied magnetic field simulation resulting formulation metrics for the 3D geometry are presented in Table II. The T-based formulations, i.e. $T-A$ and $T-\phi$, correspond to the fastest, approximately 18.17 times and 62.96 times faster than the H formulation, respectively.

The applied transport current simulation resulting formulation metrics for the 3D geometry are presented in Table III. The T-based formulations, i.e. $T-A$ and $T-\phi$, correspond to the fastest, approximately 19.06 times and 46.62 times faster than the H formulation, respectively.

The instantaneous Joule losses P for the 3D geometry, presented in Figure 5, also show similar solutions across formulations. Some deviations are verified between H and $H-A$, $T-A$ and $T-\phi$, as well as $H-\phi$, which are not only consequence of the mesh used, but also of the current density deviations, specifically between the H-based and T-based formulations.

The T-based formulations are considered to be the ones that more accurately represent a real HTS tape, in what regards its thickness, since the simplified model considerably impacts the current density $\mathbf{J}$ distribution results accuracy (with respect to a real-thickness HTS tape model).

The $T-\phi$ formulation has a high potential, being even faster than the $T-A$ formulation in 3D geometries. However, it has some disadvantages, not only the ϕ formulation drawbacks regarding the impossibilities of the thin cuts definition in some geometries and the convergence problems given small Ω_ϕ regions, but also because the meshing has shown to be a very arduous task, i.e. convergence is only obtained when a very specific meshing is done, which may represent a considerable impediment in simulating the geometries of interest.

[1] https://drive.google.com/drive/folders/1YfTsbMRJ0a-VHJYZaCuHyaPkkW-5xnoU?usp=sharing

Table II: HTS tape stack 3D applied magnetic field simulation formulation metrics

Formulation	No. Elements			DOFs	RAM	Computation Time	Normalized
	Domain	Boundary	Edge		[GB]	[hh:mm:ss]	Speed
H	30 374	10 082	1284	196 478	8.67	04 : 19 : 10	1
$H-A$				174 068	9.69	05 : 52 : 20	0.74
$H-\phi$	62 263	17 728	1645	253 568	5.98	04 : 24 : 41	0.98
$T-A$	20 649	5674	661	135 794	5.05	00 : 14 : 16	18.17
$T-\phi$	25 355	2806	673	49 825	3.67	00 : 04 : 07	62.96

Table III: HTS tape stack 3D applied transport current simulation formulation metrics

Formulation	No. Elements			DOFs	RAM	Computation Time	Normalized
	Domain	Boundary	Edge		[GB]	[hh:mm:ss]	Speed
H	30 214	10 082	1284	196 478	8.62	06 : 46 : 22	1
$H-A$				174 068	9.32	05 : 24 : 23	1.25
$H-\phi$	69 464	20 286	2378	281 505	7.39	07 : 06 : 29	0.95
$T-A$	20 649	5674	661	135 794	4.84	00 : 21 : 19	19.06
$T-\phi$	29 319	4798	830	58 748	3.87	00 : 08 : 43	46.62

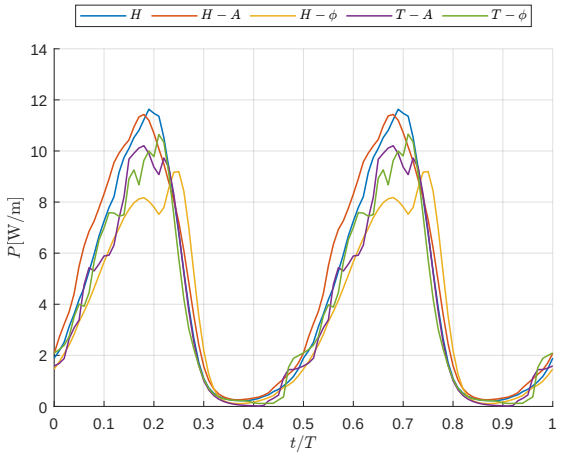

Figure 5: HTS tape stack applied transport current simulation losses

The $T-A$ formulation has shown good solution results, being reliable, versatile, computational resource efficient, and overall advantageous in both 2D and 3D geometries. Therefore, the $T-A$ formulation corresponds to the one selected in this work to simulate more complex HTS tape topologies.

C. HTS TSTC Cable

The HTS TSTC corresponds to an HTS tape stack which is twisted along the cable length, obtaining partial tape transposition.

A representative view of the geometry used, without the air geometry, is presented in Figure 6.

Accordingly, the six tape HTS TSTC geometry implemented in FEM software corresponds to a portion of an infinitely-long cable, whose HTS tapes have the dimensions previously stated, i.e. $w_{tape} = 4\,\mathrm{cm}$ and $h_{tape} = 95.6\,\mu\mathrm{m}$, and a length of

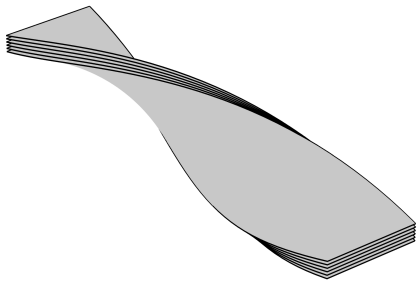

Figure 6: HTS TSTC cable geometry, without the air domain

$l_{tape} = 2\,\mathrm{cm}$. In the stack, each HTS tape is separated by air from the corresponding neighbors by a distance of $d_{tapes} = 0.5h_{tapes} = 47.8\,\mu\mathrm{m}$. Moreover, the stack is twisted so that a 180° twist is verified after a cable length of $l_{tape} = 2\,\mathrm{cm}$. A cylinder with a radius of $r_{air} = 1.5\,\mathrm{cm}$ and centered in the geometric center of the cable is used to involve the cable in air.

The simulation results regarding the mesh, DOFs, RAM usage, and computation time are presented in Table IV.

Table IV: HTS TSTC cable applied transport current simulation metrics

No. Elements			DOFs	RAM	Computation time
Domain	Boundary	Edge		[GB]	[hh:mm:ss]
49 818	12 594	1016	331 312	8.43	02 : 21 : 57

The behavior of both magnetic flux density distribution in Ω_{air} and current density distribution in Ω_{HTS} is similar to the behavior result of the HTS tape stack applied transport current simulation, being different in the magnetic flux density distribution, which is now "twisted" alongside the TSTC cable longitudinal length.

Two representative field distribution results are presented in Figures 7 and 8, namely of the current density J distribution at the simulation time instant $t/T = 0$ and of the magnetic flux density B distribution at the simulation time instant $t/T = 0.25$, respectively (more in the Google Drive folder).

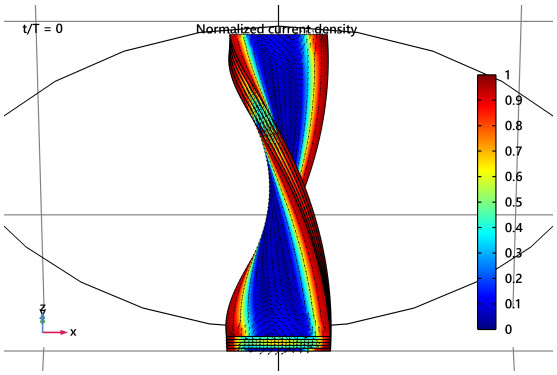

Figure 7: HTS TSTC cable applied transport current simulation $T - A$ formulation current density distribution result at the simulation time instant $t/T = 0$

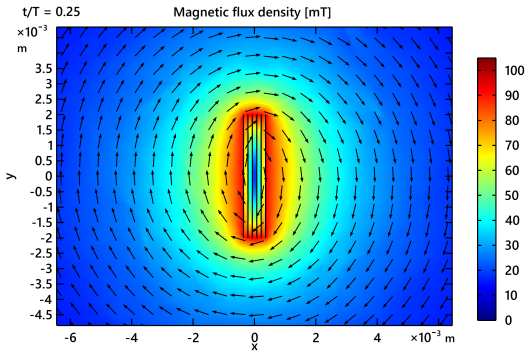

Figure 8: HTS TSTC cable applied transport current simulation $T - A$ formulation magnetic flux density distribution result at the simulation time instant $t/T = 0.25$

The maximum magnitude of the magnetic flux density occurs at the simulation time instant $t = 0.25\,\mathrm{s}$ and around the surface of the outer HTS tapes, with the value of $B_{max} \approx 100\,\mathrm{mT}$.

The instantaneous Joule losses P, presented in Figure 9, also show a similar shape to the results from the HTS tape stack simulation. The instantaneous Joule losses peak value, corresponding to $P_{max} \approx 20\,\mathrm{W\,m^{-1}}$, is higher than the losses peak value obtained in the HTS tape stack simulation ($P_{max}^{stack} \approx 12\,\mathrm{W\,m^{-1}}$).

These losses values, as well as the values for the magnetic flux density norm, cannot be directly compared with the HTS tape stack simulation, since the gap distance between tapes is not the same: in the tape stack $d_{tapes} = 2h_{tape}$ and in the TSTC cable $d_{tapes} = 0.5h_{tape}$. In fact, since the distance between tapes is smaller in the TSTC cable, the critical current J_c in the tapes is smaller (given the higher field effects between tapes), and, consequently, losses will be higher for the same transport current.

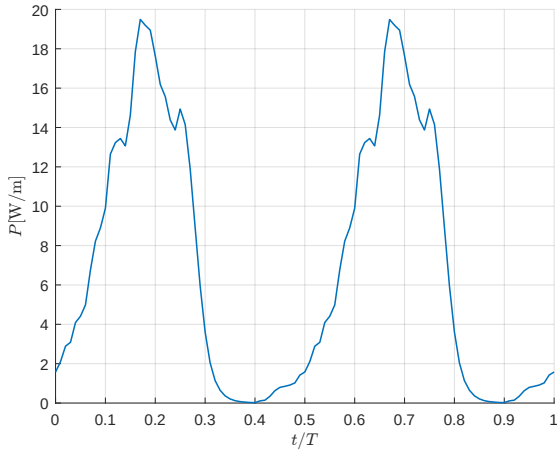

Figure 9: HTS TSTC cable applied transport current simulation losses

D. HTS CORC Cable

The HTS CORC cable corresponds to a cable containing HTS tapes arranged helically around a cylindrical former in one or several layers.

A representative view of the solution geometry used, without the air geometry, is presented in Figure 10.

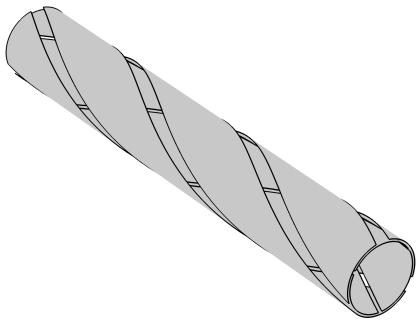

Figure 10: HTS CORC cable geometry, without the air domain

Accordingly, the six tape HTS CORC cable geometry implemented in FEM software corresponds to a portion of an infinitely-long cable, whose HTS tapes have the dimensions previously stated, i.e. $w_{tape} = 4\,\mathrm{cm}$ and $h_{tape} = 95.6\,\mu\mathrm{m}$, and a length of $l_{tape} = 2\,\mathrm{cm}$. In this CORC topology, two layers of three tapes each are considered. In the most inner layer, the three tapes are arranged in a cylindrical surface so that an angle of 3° separates each tape. Moreover, the outer layer is separated from the inner layer by a radial distance of $d_{tapes} = 0.5h_{tapes} = 47.8\,\mu\mathrm{m}$, with its tapes equally distributed along that outer layer cylindrical surface. The twist of each layer is done so that a 360° twist is verified after a cable length of $l_{tape} = 3\,\mathrm{cm}$, with the inner and outer layers tapes being twisted in opposite directions. A cylinder with a radius of $r_{air} = 1.5\,\mathrm{cm}$ and centered in the geometric center of the cable is used to involve the cable in air.

In contrast with all other geometries studied so far, in the CORC geometry, the natural boundary conditions and other added constraints are not enough to guarantee the periodicity of the solution, and no method of constraining a periodicity

condition was neither found in the literature nor developed in the course of this work.

Therefore, a solution truncation method is used, i.e. the geometry considered in the FEM software has a total length of $4/3$ the initial length ($4\,\mathrm{cm}$). After the simulation is conducted, the intended solution is extracted from the full solution by disregarding $1/6$ ($0.5\,\mathrm{cm}$) of the initial length from each side of the whole geometry. This method, as expected, has shown to deliver the intended periodic solution for the HTS CORC cable.

The simulation results regarding the mesh, DOFs, RAM usage, and computation time are presented in Table V.

Table V: HTS CORC cable applied transport current simulation metrics

No. Elements			DOFs	RAM	Computation time
Domain	Boundary	Edge		[GB]	[mm:ss]
52 506	11 074	1374	346 178	8.17	52 : 06

It is interesting to notice that, even though the same number of HTS tapes is considered and an equivalent applied transport current simulation is conducted in both TSTC and CORC geometries, the latter geometry simulation is about 2.7 times faster than the former. In fact, using the $T-A$ formulation, and the differences regarding the solution truncation method used, the proposed CORC geometry leads to a higher convergence of the numerical method when compared to the proposed TSTC geometry.

The behavior of both magnetic flux density distribution in Ω_{air} and current density distribution in Ω_{HTS} correspond to the expected. A circular magnetic flux density distribution is verified around the cable, being uniform alongside its length, and with the magnetic flux density inside the cable being approximately null. This circular magnetic flux density outside the cable and the shielding effect inside it are a consequence of the distribution of the HTS tapes in the cylindrical former.

Two representative field distribution results are presented in Figures 11 and 12, namely of the current density J distribution at the simulation time instant $t/T = 0.15$ and of the magnetic flux density B distribution at the simulation time instant $t/T = 0.25$, respectively (more in the Google Drive folder).

In addition, it is verified that the layer mainly responsible for the current transport is the inner one. In fact, given the magnetic flux density shielding, the inner HTS CORC layer feels a lower magnetic flux density magnitude, and, consequently, its tapes critical current J_c is higher than the one from the outer layer. Moreover, and as expected, there is no difference in both the magnetic flux density distribution in Ω_{air} and current density distribution in Ω_{HTS} not only along the length of the cable, but also from tapes of the same layer, since, as a consequence of the symmetry, all tapes within a layer are in the same conditions regarding the electromagnetic fields.

The maximum magnitude of the magnetic flux density occurs at the simulation time instant $t = 0.25\,\mathrm{s}$ and around the surface of the outer HTS tapes, with the value of $B_{max} \approx 60\,\mathrm{mT}$, corresponding to a value approximately 1.67

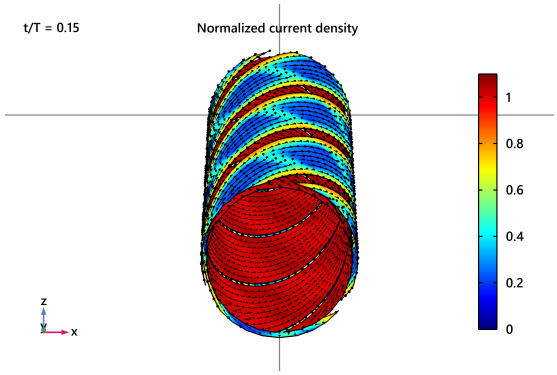

Figure 11: HTS CORC cable applied transport current simulation $T-A$ formulation current density distribution result at the simulation time instant $t/T = 0.15$

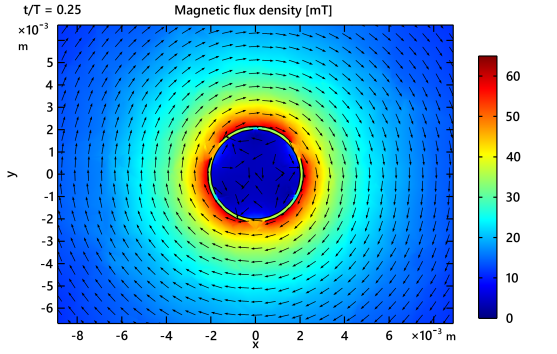

Figure 12: HTS CORC cable applied transport current simulation $T-A$ formulation magnetic flux density distribution result at the simulation time instant $t/T = 0.25$

times lower than the one obtained in the HTS TSTC cable simulation.

The instantaneous Joule losses, presented in Figure 13, show a similar shape to the results from the HTS TSTC cable simulation. The instantaneous Joule losses peak value, corresponding to $P_{max} \approx 3\,\mathrm{W\,m^{-1}}$, is 6.67 times lower than the losses peak value obtained in the HTS TSTC cable simulation ($P_{max}^{stack} \approx 20\,\mathrm{W\,m^{-1}}$).

In both HTS TSTC cable and HTS CORC cable simulations, the total transport current is the same, and, despite the lower maximum magnetic flux density magnitude value obtained in the HTS CORC topology when compared to the HTS TSTC topology, its distribution around the cable is more uniform, being, in fact, circular, similarly to the magnetic flux density distribution obtained using round wires, even though rectangular-shaped conductors are used, specifically HTS tapes. This magnetic flux density distribution may be desirable in certain applications, e.g. in high magnetic field applications. Additionally, the Joule losses are considerably lower in the HTS CORC cable, making it more interesting efficiency-wise.

IV. Conclusions

The objectives set for this thesis were almost globally met, with the exception of some, which were not fulfilled, given

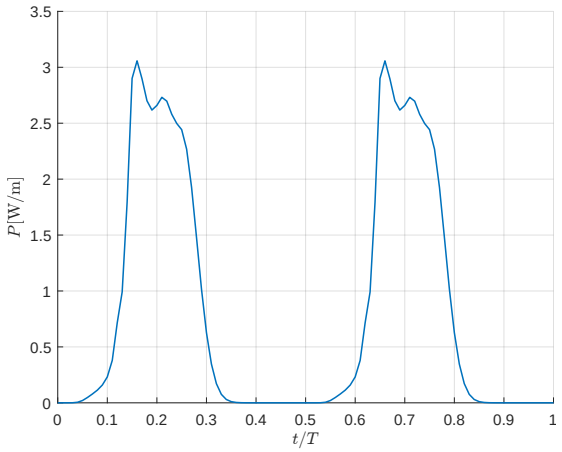

Figure 13: HTS CORC cable applied transport current simulation losses

the limited time available.

The electromagnetic formulations used to simulate HTS-CC and HTS tape topologies proposed in the literature were reviewed and the respective implementations in FEM software were studied.

In the case of some formulations, extensively described in the literature, e.g. the H formulation, the respective implementation review was straightforward. However, for other formulations, specially regarding the $T-A$ formulation, the literature implementation proposals were often lacking information or were merely superficial. Therefore, for these cases, a more in-depth study was conducted and the consequent implementation aspects proposed. Additionally, in the particular case of the $T-\phi$ formulation, the information found in the literature was scarce and even failed on providing outlines for its FEM software implementation. In the course of this work, the $T-\phi$ formulation FEM software implementation was developed and proposed.

Different FEM software models were developed for different HTS tape topologies and simulations, namely applied magnetic field and applied transport current simulations, including the studied formulation implementation templates. The developed models and templates, which are delivered with this thesis, are general enough to, alongside the described formulation implementations, be used in different simulation conditions than the ones developed, e.g. applied transport current under a background magnetic field.

Finally, the advantages and disadvantages, as well as the strengths and limitations of each studied electromagnetic formulation were analyzed, following the simulations developed and the respective obtained results.

The $T-A$ formulation has shown to be the most interesting to simulate HTS tape topologies in FEM, being, among the studied, the most reliable, versatile, and computational resource efficient. Moreover, its inherent approximation of the HTS tape as a thin sheet has delivered accurate results, specifically regarding current density distributions in the HTS layer.

Nevertheless, in the course of this work, several obstacles were encountered. The most notorious corresponding to the evident lack of information in the literature regarding the implementation of the $T-A$ formulation in HTS tape topologies. In fact, while some of the gaps were filled throughout this work, others, specifically regarding the implementation of periodic conditions, were left blank. As a consequence, other HTS tape topologies, e.g. RACC cable, were not simulated, even though FEM software geometries were developed with such purpose.

Acknowledgements

The author would like to acknowledge the indispensable support of all the people in the Electrical Machines Laboratory, in special Eng. Francisco Ferreira da Silva and Prof. Paulo José da Costa Branco.

References

[1] T. P. Sheahen, *Introduction to High-Temperature Superconductivity*. Kluwer Academic Publishers, 1994.

[2] A. V. Narlikar, *High Temperature Superconductivity 2*. Springer, 2004.

[3] J. V. Yakhmi, *Superconducting Materials and Their Applications: An interdisciplinary approach*. IOP Publishing Ltd, 2021.

[4] Super Power Inc., *2G HTS Wire Specification*, [Online]. Available: https://superpower-inc.com/specification.aspx

[5] Z. Hong and A. M. Campbell and T. A. Coombs, "Numerical solution of critical state in superconductivity by finite element software", in *Superconductor Science and Technology*, vol. 19, no. 12, pp. 1246–1252, 2006. DOI: 10.1088/0953-2048/19/12/004.

[6] V. M. R. Zermeno and F. Grilli and F. Sirois, "A full 3D time-dependent electromagnetic model for Roebel cables", in *Superconductor Science and Technology*, vol. 26, no. 5, pp. 052001, 2013. DOI: 10.1088/0953-2048/26/5/052001.

[7] F. Gömöry and M. Vojenčiak and E. Pardo and J. Šouc, "Magnetic flux penetration and AC loss in a composite superconducting wire with ferromagnetic parts", in *Superconductor Science and Technology*, vol. 22, no. 3, pp. 034017, 2009. DOI: 10.1088/0953-2048/22/3/034017.

[8] S. Mykola and G. Fedor, "A–V formulation for numerical modelling of superconductor magnetization in true 3D geometry", in *Superconductor Science and Technology*, vol. 32, no. 11, pp. 115001, 2019. DOI: 10.1088/1361-6668/ab3a85.

[9] L. Bortot and B. Auchmann and I. C. Garcia and H. D. Gersem and M. Maciejewski and M. Mentink and S. Schöps and J. V. Nugteren and A. P. Verweij, "A Coupled A-H Formulation for Magneto-Thermal Transients in High-Temperature Superconducting Magnets", in *IEEE Transactions on Applied Superconductivity*, vol. 30, no. 5, pp. 1–11, 2020. DOI: 10.1109/TASC.2020.2969476.

[10] R. Brambilla and F. Grilli and L. Martini and M. Bocchi and G. Angeli, "A Finite-Element Method Framework for Modeling Rotating Machines With Superconducting Windings", in *IEEE Transactions on Applied Superconductivity*, vol. 28, no. 5, pp. 1–11, 2018. DOI: 10.1109/TASC.2018.2812884.

[11] A. Arsenault and F. Sirois and F. Grilli, "Implementation of the H-ϕ Formulation in COMSOL Multiphysics for Simulating the Magnetization of Bulk Superconductors and Comparison With the H-Formulation", in *IEEE Transactions on Applied Superconductivity*, vol. 31, no. 2, pp. 1–11, 2021. DOI: 10.1109/TASC.2020.3033998.

[12] A. Arsenault and B. S. Alves and F. Sirois, "COMSOL Implementation of the H-ϕ-Formulation With Thin Cuts for Modeling Superconductors With Transport Currents", in *IEEE Transactions on Applied Superconductivity*, vol. 31, no. 6, pp. 1–9, 2021. DOI: 10.1109/TASC.2021.3097245.

[13] E. Berrospe-Juarez and V. M. R. Zermeño and F. Trillaud and F. Grilli, "Real-time simulation of large-scale HTS systems: multi-scale and homogeneous models using the T–A formulation", in *Superconductor Science and Technology*, vol. 32, no. 6, pp. 065003, 2019. DOI: 10.1088/1361-6668/ab0d66.

[14] H. Zhang and M. Zhang and W. Yuan, "An efficient 3D finite element method model based on the T–A formulation for superconducting coated conductors", in *Superconductor Science and Technology*, vol. 30, no. 2, pp. 024005, 2016. DOI: 10.1088/1361-6668/30/2/024005.